Crystal Structure of Recombinant Human Platelet Factor 4

Xiaohua Zhang,*,‡ Liqing Chen, and Daniel P. Bancroft§

Department of Biology, Massachusetts Institute of Technology, Cambridge, Massachusetts 02139

C. K. Lai and Theodore E. Maione

Repligen Corporation, One Kendall Square, Building 700, Cambridge, Massachusetts 02139

Received July 15, 1993; Revised Manuscript Received April 4, 1994®

ABSTRACT: The crystal structure of human platelet factor 4 (PF4) has been solved to a resolution of 2.4 Å by molecular replacement and refined to an *R*-factor of 24.1%. The structure consists of four polypeptide chains which form a tetrameric unit. N-terminal residues, previously defined as a random coil or extended loop region, form antiparallel β-sheet-like structures that form noncovalent associations between dimers. These antiparallel β-sheet-like structures are positioned lateral to the β-bilayer motif and stabilize the tetrameric unit. A positively charged ring of lysine and arginine side chains encircles the PF4 tetramer sphere, presenting multiple potential sites and orientations for heparin binding. The electrostatic interactions of multiply charged amino acid side chains and hydrogen bonding interactions at the AB/CD dimer interface serve to stabilize the tetrameric structure further.

Platelet factor 4 (PF4)[1] in mammalian species is localized in the α-granules of platelets bound to a high molecular weight proteoglycan rich in chondroitin sulfate (Broekman, 1975; Barber, 1972). Following platelet activation, α-granule contents are released. PF4 belongs to a large superfamily of the cytokines (IL-8, NAP-2, Gro-α, etc.) referred to as intercrines or chemokines which are proteins involved in the immune and inflammatory responses and in the mediation of cell growth (Matsushima & Oppenheim, 1989). Despite the amino acid sequence homology of these cytokines, they appear to possess distinct biological properties.

Although the physiological role of PF4 is poorly defined, a number of biological activities have been reported for this protein (Katz et al., 1986; Zucker et al., 1989). PF4 demonstrated immunoregulatory activities in the reversal of Con A or γ-irradiated lymphoma-induced immunosuppression in mice. Complementary in vitro studies led to the interpretation that these effects represented modulation of T-cell-mediated immunity by PF4. It also appears to selectively inhibit binding of transforming growth factor β_1 to its receptor (Whitson et al., 1991) and may be chemotactic for neutrophils and monocytes (Deuell et al., 1981) at doses significantly higher than required for the other active chemokines. PF4 was first characterized by its high affinity for heparin (Handin & Cohen, 1976), a clinically important blood anticoagulant which consists of sulfated polysaccharides containing a linear polymer of glucosamine and uronic acid. Its ability to neutralize the anticoagulant properties of heparin has been clearly demonstrated in vitro (Lane et al., 1984; Michalski et al., 1978; Hunt et al., 1990) and in vivo (Cook et al., 1992). Purified recombinant PF4 has also been shown to inhibit angiogenesis in vivo and endothelial cell proliferation in vitro (Maione et al., 1990). Subsequent studies demonstrated the ability of rPF4 to inhibit tumor growth in vivo, by a T-cell-independent mechanism and without direct effects on the tumor cells in vitro (Sharpe et al., 1990), probably as a result of suppression of tumor-induced neovascularization. These studies have been further extended to demonstrate significant inhibition in the development of B16F10 melanoma lung metastases by systemic administered recombinant human PF4 (Kolber & Maione, 1992) by a similar mechanism. In view of these pleiotrophic activities, detailed evaluation of crystallographic data for these cytokines and correlation of their primary structural differences with their respective activities could provide important information concerning receptor binding domains, active sites, and physiological roles.

The monomer of human PF4 consists of 70 amino acids with a molecular mass of 7766 daltons and is identical in sequence to recombinant human PF4 reported previously and used in these studies (Hermodson et al., 1977; Morgan et al., 1977; Walz et al., 1987). Under physiological conditions, four identical polypeptide chains assemble in a defined manner, and it is assumed that the tetramer is the active form of PF4 in biological systems. Human PF4 is 70% homologous with bovine PF4, for which the structure has been solved to 3.0 Å (R = 28.0%; St. Charles et al., 1989). For those studies, bovine PF4 was first treated with porcine elastase to remove the first 13 amino acids from the amino terminal, which appeared necessary to promote crystallization. This domain was also suggested to include an oligosaccharide. Furthermore, the $Ni(CN)_4^{2-}$ complexes used to crystallize bovine PF4 are assumed to distort the true electrostatic interaction within the AB/CD tetrameric interface, confounding the interpretation of the true physical significance of the model proposed.

Currently, there is no evidence that the human form of PF4 contains covalently linked carbohydrate side chains nor is proteolytic treatment required for its crystallization. Hence, solving the high-resolution crystal structure of recombinant human PF4 was expected to yield a more accurate representation of its native structure.

It has been reported that human heparin is structurally similar to porcine heparin but is remarkably different from

* Address correspondence to this author.

‡ X.Z. was a fellow of International Human Frontier Science Program Organization in 1991–1992.

§ Present address: Department of Biochemistry, School of Medicine, University of Utah, Salt Lake City, UT 84132.

® Abstract published in *Advance ACS Abstracts,* June 15, 1994.

[1] Abbreviations: PF4, platelet factor 4; IL-8, interleukin 8; NAP-2, neutrophil activating peptide-2; Gro-α, growth-related gene product; bFGF, basic fibroblast growth factor.

0006-2960/94/0433-8361$04.50/0

Table 1: X-ray Data Collection

parameter	overall (8–2.4 Å)	resolution shells (Å) 8.0–4.53	4.53–3.71	3.71–3.28	3.28–3.0	3.0–2.79	2.79–2.63	2.63–2.51	2.51–2.4
unique reflections measured ($F > 2\sigma$)	11037	1514	1467	1450	1415	1340	1351	1298	1202
% complete ($F > 2\sigma$)	94.4	99.0	98.8	99.0	98.2	91.5	91.4	95.9	81.5
R_{merge}[a] (%)	6.05								

[a] $R_{merge} = \sum_i |\langle I_i \rangle - I_i| / \sum_i I_i$ and $\langle I_i \rangle$ is the average of I_i over all symmetry equivalents.

the bovine form (Linhardt et al., 1992). The structural variation of heparin from different species could lead to evolutionary differences in the PF4 strutures and in the mode of interactions of these heparins with their respective PF4. The crystal structure of human PF4 should represent a more accurate model for studying human heparin–PF4 interactions than the bovine form. Several models have been proposed to explain the high affinity of PF4 with heparin (Luscombe & Holbrook, 1983; Denton et al., 1983; Ibel et al., 1986; Cowan et al., 1986), but conclusive structural data have not yet been reported. A well-resolved structure of human PF4 would facilitate elucidation of the poorly understood PF4–heparin binding mechanism. In this paper, we identify key structural features of human PF4 differing from the modified bovine protein and discuss their relevance to high-affinity heparin binding and stabilization of the tetrameric structure.

MATERIALS AND METHODS

Protein Purification and Crystal Growth. Recombinant human PF4 was isolated as a fusion protein expressed in *Escherichia coli*. The protein was purified, cleaved, and refolded as previously described (Myers et al., 1991), yielding a protein of identical amino acid sequence to human platelet-derived PF4. A combination of ion-exchange and gel filtration columns was used to remove the acetonitrile/aqueous trifluoroacetic acid buffer from earlier HPLC steps. The highly purified rhPF4 (12 mg/mL) in 10 mM sodium acetate and 150 mM sodium chloride at pH 5.0 was used for crystallization. Crystals were grown by the hanging-drop vapor-diffusion method at 20 °C. A 2-μL sample of protein solution was resuspended over a reservoir containing the same buffer as the protein solution. The pH of the reservoir solution had been adjusted to 7.9 by NH_4OH. Crystals formed after 1–2 days. The crystals used for data collection measured approximately 0.8 × 0.4 × 0.1 mm.

Data Collection. Recombinant human PF4 crystallizes in the orthorhombic space group $P2_12_12_1$ with unit-cell dimensions of $a = 78.2$, $b = 86.2$, and $c = 43.4$ Å. X-ray diffraction intensities were measured and processed with the use of the R-axis II imaging plate system (Molecular Structure Corp.). Data were collected at room temperature for a total of 80 frames in 2 orientations with a 2.5° oscillation angle and a crystal to frame distance of 110 mm. The parameters of data collection are listed in Table 1.

Rotation and Translation Searches. Rotation and translation function searches were performed using the program package MERLOT (Fitzgerald, 1988). An initial estimation, based on the ratio of the molecular weight to the unit-cell volume, suggested one PF4 tetramer per asymmetric unit. The coordinates from the tetrameric unit of bovine PF4 were used in the initial search (St. Charles, personal communication). The model was placed in an arbitrary 120 × 120 × 120 Å P_1 orthogonal unit cell, and structure factors were calculated to 3.5-Å resolution. The Euler angle search range for cross-rotation peaks was as follows: α, 0–180°; β, 0–90°; γ, 0–360°, using a coarse grid of 5.0°, a radius of integration of 22 Å, and resolution limits between 8 and 3.7 Å. The highest peak (6.1σ) was found at $\alpha = 3.57°$, $\beta = 5.92°$, and $\gamma = 114.11°$, and was considered as a tentative solution. The rotation angles were then refined using the Lattman rotation function (Lattman & Love, 1972).

The translation function of Crowther and Blow (1967) was used to determine the translation components along the three axes for the unknown molecule in the $P2_12_12_1$ unit cell. The translation function results gave distinct peaks ($\sim 6.1\sigma$) in the Harker sections corresponding to the A–A′ intermolecular vectors for resolution ranges between 8 and 3.7 Å. The corresponding translation vectors were $x = 0.21$, $y = 0.15$, and $z = 0.42$. The initial model was rotated and translated according to the solution and subsequently refined by *R*-factor minimization to an *R*-factor of 0.39 (8–3.5 Å). The crystal packing was then checked to reveal any inappropriate intermolecular contacts.

Refinement. The refinement of the molecular replacement model was carried out at 8–2.4-Å resolution using the program package XPLOR (Brunger, 1989) with 11 037 total unique reflections. The tetramer was initially refined as one rigid body followed by a refinement which grouped the four polypeptide chains as individual rigid bodies. This reduced the *R*-factor by about 1.5%. The atomic positions were then refined with the simulated annealing routine in XPLOR. Finally, the tetramer was refined a total of 160 cycles of conjugate gradient energy minimization which reduced the *R*-factor to 28%. At this stage, omit maps of $2F_o - F_c$ and $F_o - F_c$ for every 10 amino acids were made for the entire molecule to replace the different residues with the human PF4 sequence. After fitting the correct amino acid residues and adjusting side chain conformations of a few other amino acid residues, the resulting model was refined by energy minimization to an *R*-factor of 26%. Additional $2F_o - F_c$ and $F_o - F_c$ maps clearly revealed the presence of extra electron density in the N-terminal region of all four subunits that were disordered in the bovine PF4 structure. Two additional amino acid residues were fitted in each subunit. The final structure includes residues 7–70 in 4 polypeptide chains. The remaining six amino acid residues in the N-termini are disordered. The final *R*-factor is 24.1% with rms bond and angle deviations of 0.016 and 3.89°, respectively. The final structure includes 91 water molecules. Ramachandran plots for the individual polypeptide chains reveal the appropriate stereochemistry (data not shown). The atomic coordinates of human PF4 are currently being submitted to the Brookhaven Protein Data Bank.

RESULTS AND DISCUSSION

The overall structure of human PF4 consists of four identical subunits with pseudo-*222* symmetry. The four subunits are defined as A, B, C, and D with residue numbers 7–70, 107–170, 207–270, and 307–370, respectively. A pseudo-2-fold symmetry is present between A and B, or C and D. A tetramer is formed by a pseudo-2-fold axis between AB and CD. A 2-fold axis is also present between A and C, or B and C.

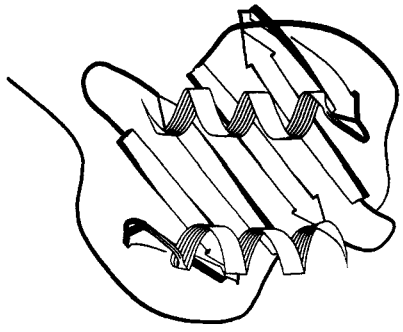

FIGURE 1: Ribbon diagram of the AB dimer.

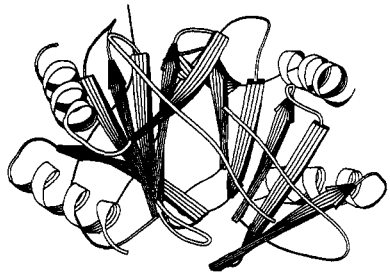

FIGURE 2: Ribbon diagram of the PF4 tetramer.

Consequently, tetramers can also be formed between AC and BD. Monomeric units start with a region of random coils or extended loop (residues 7–24) followed by a three-strand antiparallel β-sheet and finish with an α-helical region which lies across the β-sheet. The monomer random-coil region is stabilized by two disulfide bonds (S=S, 2.01 Å, Cys-10 to Cys-36; 1.99 Å, Cys-12 to Cys-52). Dimers (AB and CD) are maintained by hydrogen bonding of the β-sheet regions in an antiparallel fashion. By this association, the structure of the complete region has a "floor", consisting of a continuous six-strand antiparallel β-sheet (Figure 1). The two helical regions above the extended β-sheet are nearly antiparallel to each other and separated by a large distance, about $\sim$13 Å, from center to center. The two dimers associate with each other through surface interactions of the β-sheets with the two pairs of α-helices located on opposite sides of the surface of the tetramer (Figure 2).

The overall structure of human PF4 is similar to the structure of bovine PF4. Superposition of Cα atoms of the two tetramers shows that the rms deviation for 248 (for residues 9–70 of 4 subunits) Cα atoms is 0.879 Å. However, more structural details were revealed with this 2.4-Å resolution model.

Residues from N-terminal regions, which were previously defined as random coil or extended loop, possess a very defined structural conformation due to interactions of N-terminal residues between the A to C and B to D dimers, respectively. Residues 7–18 of monomer A and C, or monomer B and D, are antiparallel to each other and form paired antiparallel β-sheet-like structures. Of the 12 hydrogen bonds at the N-termini of the BD dimer, 6 formed β-sheet-type hydrogen bonds between residues 107–114 and 307–315 (Figure 3). Thirteen hydrogen bonds are observed in β-sheet-like structures of the AC dimer. Most of the hydrogen bonds occur between the atoms of side chains or between the atoms of side chains and backbones. Some of these hydrogen bonds are bridged by water molecules. For example, water 289 can be observed to bridge residues 14 and 15 to 211 by a total of 4 hydrogen bonds. Water 186 bridges 17, 54, and 109 together. These N-terminal residues with β-sheet-type hydrogen bond interactions are positioned lateral to the β-bilayer motif and contribute significant energy to the interaction between dimers AC and

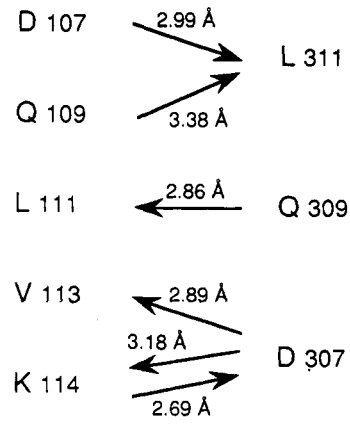

FIGURE 3: Hydrogen bonding scheme of the β-sheet structure in the N-termini of the BD dimer. The arrow points to the direction in which a hydrogen bond is formed from a nitrogen to an oxygen atom.

BD forming the ultimate tetramer structure. Therefore, the tetrameric structure of PF4 is stabilized not only by salt bridge interactions between dimers AB/CD, which were previously identified as the major stabilizing force in the tetramer structure, but also by the β-sheet-like structure in the N-termini of dimers AC or BD.

The high-resolution structure of PF4 also more precisely defined the structural features at the β-sheet interface of the PF4 tetramer. Salt bridges can be formed from four pairs of charged residues located on the β-sheet surface. The distances of Glu-OE1 to Lys-NZ for salt bridge pairs Glu-28/Lys-250 (A/C) and Glu-228/Lys-50 (C/A) are 2.84 and 3.68 Å, respectively. Inspection of electron density maps at the tetramer β-sheet region revealed that three types of interactions are involved in this energy stabilization of the tetrameric molecule. These interactions include electrostatic interaction, hydrogen bonding, and van der Waals forces; however, the dominating energy forces are produced by electrostatic and hydrogen bonding interactions. The side chains of six residues from each monomer (Thr-25, Ser-26, Glu-28, Gln-40, Thr-44, and Lys-50) contributed heavily to hydrogen bonding, and two residues (Ile-30 and Ile-42) contributed to van der Waals contacts. These hydrogen bonds form either within a monomer or between monomers and flank the salt bridge atoms or are bridged with water molecules to facilitate the electrostatic interaction and, consequently, stabilize the tetramer. The hydroxyl group of threonines and serines plays a particularly important role on the hydrogen bonds in this region. The electrostatic interactions in BD dimer residues are weaker than those in AC dimers. The distances of the two pairs of potential salt bridge atoms from monomers B and D (Glu-128/Lys-350 and Glu-328/Lys-150) are 8.07 and 8.63 Å, respectively. The failure to form salt bridges in dimer B/D was previously reported in the bovine PF4 structure and was assumed to be the result of the distortion caused by the nickel substitution (St. Charles et al., 1989). Since the human PF4 crystals do not require heavy atom substitution, the lack of salt bridges in the BD dimer probably represents the intrinsic arrangement of tetramer subunits following energy minimization based on energy compensation within the tetramer unit. The electrostatic interaction can be accommodated by solvent molecules in the β-sheet interface region. Electron densities are observed among the salt bridge and side chains atoms of hydrophilic residues across the BD dimer. These observations suggest that additional solvent molecules facilitate the electrostatic and hydrogen bonding interactions in the BD dimer.

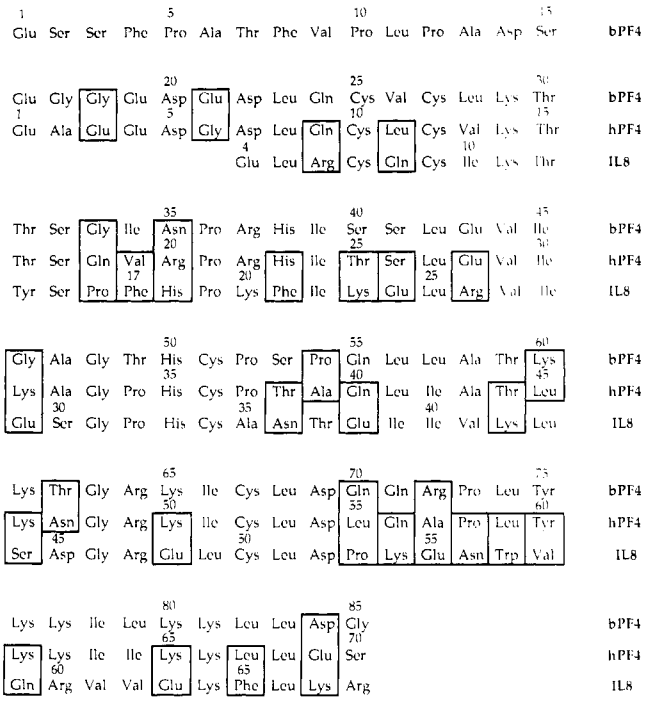

FIGURE 4: Amino acid sequences of bovine and human PF4 and interleukin 8. Framed amino acids represent the nonconserved sequential changes.

Besides β-sheet hydrogen bonds, dimers are stabilized by interactions between the α-helix and β-sheet or nearby loops. The α-helices of PF4 are amphipathic. The hydrophobic residues of the α-helix interact with the β-sheet and the N-terminal β-sheet-like regions. Specific hydrophobic interactions are observed to occur between the side chains of Leu-59/Ser-17, Ile-63/Ile-24, and Leu-67/Leu-27. Other major interactions occurred at the C-terminus of the α-helical region, specifically with Glu-69 and Ser-70, which formed a total of six hydrogen bonds with the β-sheet and nearby loop residues and functioned as anchor residues for the α-helix to maintain its orientation on the surface of the β-sheets. In the previous report of bovine PF4 structure, Ser-70 was mistaken as glycine, and, as a result, the hydrogen bonding interaction could not be identified. The resequencing of bovine PF4 has recently corrected this residue to serine (St. Charles, personal communication).

The largest deviations between bovine and human PF4 structures are observed at the loop regions (other than the terminal residues). The smallest differences are observed at the β-sheet regions. The loop residues of 18–19 and 56–58 from all 4 subunits have maximal deviations of 2.99 and 2.57 Å, respectively, and are the most flexible. The loops around residues 18, 34, and 56 are positioned outside of the PF4 sphere and have maximum solvent accessibility. The others are partly buried to varying extents within the PF4 sphere, and therefore are less accessible to solvent. The loop residues 56–58 are N-terminal to the α-helixes, and loop 18–19 is positioned around a high density of positively charged residues. The PF4–ligand interactions may be facilitated by these flexible loops.

The basic tertiary structural motif of interleukin 8 is similar to that of PF4 [the X-ray model (Baldwin et al., 1991); the NMR model (Clore et al., 1990)]. The former, however, functions as a dimer instead of as a tetramer as in the case of PF4. By examining the sequence of both proteins (Figure 4), the most notable sequence differences are at residues such as Thr-25, Ser-26, Glu-28, Thr-44, and Lys-50, which significantly contribute to electrostatic interaction and hydrogen bonding interactions within the PF4 tetramer. These residues have been replaced by highly charged residues. For example, residues Ser-26, Glu-28, and Lys-50 in PF4 have been interchanged to Glu-24, Arg-26, and Glu-48 in interleukin-8, respectively. Glu-24 contributed from monomer B of IL-8, a 2-fold symmetric molecule, which formed a salt bridge with Arg-26 within the dimer and diminished the possibility of forming the salt bridge Glu-28/Lys-50 between the AC dimer in PF4. Totally, four pairs of salt bridges are formed within the IL-8 dimer. Other salt bridge pairs are formed between Glu-29/Arg-68. The charge neutralization within the dimer both stabilizes the dimer formation of IL-8 and diminishes the possibility of forming electrostatic interactions between dimers. Therefore, tetramer formation seems unlikely in interleukin 8. Since the tetramer-inducing structures of PF4 are not necessary for the functions of IL-8, the amino acid residues to maintain the tetramer structure are not rigidly conserved in IL-8 (Figure 4).

Superposition of Cα atoms of interleukin 8 (the X-ray model) with PF4 (Figure 5) produces an rms deviation for 62 Cα atoms (residues 6–68, exclude Lys-15) of 2.44 Å. The β-sheet region and disulfide linkage, which support the tertiary structure, correlate well with the PF4 structure and with a maximum shift around 2.4 Å. However, the maximum deviation was observed in the C-terminal α-helical region (4–5 Å). The large differences between the α-helices of the two proteins can be expected due to large sequence differences between these seven amino acid residues proceeding α-helices (residues 53–59, Figure 4). It seems that IL-8 retained specific PF4 structural motifs needed to support its functional domains but mutated other portions not required. Since the NMR and X-ray models of interleukin 8 are similar, the comparison above the X-ray model of interleukin 8 with that of human PF4 may also be applicable to the NMR model.

As mentioned in previous publications, the four-lysine cluster (Lys-61, Lys-62, Lys-65, and Lys-66) in the C-terminus of the α-helix is required for heparin binding. However, for efficient heparin–PF4 interactions, previous results (Ibel et al., 1986; Bock et al., 1980) suggested that, at least, 4 tetrasaccharides (16 units) were needed. All positively charged residues (Lys and Arg) of human PF4 form a positively charged ring within the tetrameric unit except Lys-14 and Lys-50 (Figure 6). The former points to the inner electrostatic core, and the latter lies approximately 25 Å from the edge of the ring. We speculate that the topology of this positively charged ring would enhance the affinity of heparin binding if the heparin–PF4 interaction is dominated by electrostatic effects. Interestingly, several additional pairs of positively charged residues from the N-terminal β-sheet-like structure are packed above or below the C-terminal lysine cluster along each side of the PF4 sphere. The Arg-220 and Arg-222 pair, from monomer C, is located within 10 Å of the lysine cluster. The other pair, Arg-320 and Arg-322, is packed on the opposite side. Thus, the arginine and lysine residues form a positively charged cluster along the PF4 sphere. Lys-31, Lys-46, and Arg-49 from the four monomers bridge the two half-spheres of the PF4 tetramer, and all lysines and arginines (except Lys-50 and Lys-14) participate in forming the positively charged domain around PF4. The positively charged ring can be further divided into two half-spheres with two antiparallel α-helices separated by the equator. Thus, the charge density is mostly distributed along the B/C or A/D half-sphere (Figure 6). The distances between neighboring charged atoms in the charge density cluster of the half-charged

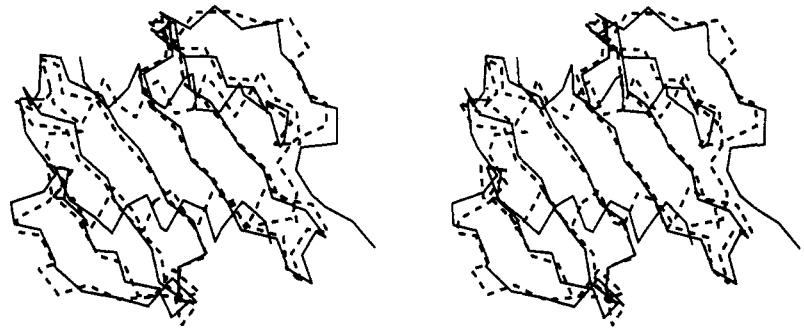

FIGURE 5: Stereo diagrams of the PF4 dimer (solid line) superimposed with the IL-8 dimer (dotted line).

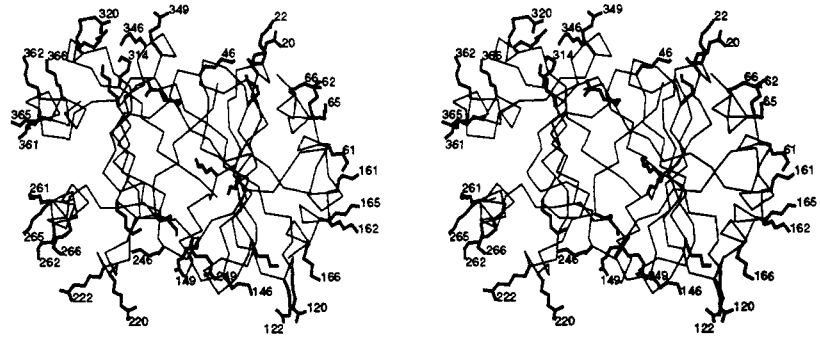

FIGURE 6: Stereoview of the PF4 tetramer with the side chains of all lysine and arginine residues except Lys-50 which involves electrostatic interactions between dimers. For clarity, not all lysine and arginine residues are labeled.

ring are mostly 8–10 Å. The cluster (Lys-261 and Lys-161) is distributed over distances of approximately 70–80 Å, and binding can be fitted roughly to a four-tetrasaccharide unit as estimated from Cowan and from Atkins et al. (about 8–8.5 Å per disaccharide, Cowan et al., 1986; Atkins & Nieduszynski, 1976). The distances between positive charges across the 2-fold helix of the positively charged ring are approximately 10 Å, which correlates well with the distances between the negative charges on the 2-fold helix of sulfated polysaccharides (~10 Å). These structural features are all consistent with the observations reported in the previous studies of heparin–PF4 interactions (Ibel et al., 1986; Bock et al., 1980). From the point of view of electrostatic interactions, we speculate that the heparin binding sites are more likely to be along the positively charged circle (at right angles across the α-helical axis) and less likely across the positively charged circle. However, a precise conclusion on whether electrostatic interactions are important in the binding mechanism of the heparin–PF4 complex will require solving a high-resolution structure of the complex.

The structural motif of the PF4 dimer has also been found in the α_1 and α_2 domains of the HLA-A2 molecule (Bjorkman et al., 1987). The crevice formed by the two parallel α-helices in HLA-A2 possesses sufficient space for a peptide with 8–20 amino acids and functions as antigen binding sites. In the case of PF4, the crevice is much smaller. No evidence for receptor binding in the PF4 α-helical region has yet been reported.

ACKNOWLEDGMENT

We acknowledge Dr. Robert St. Charles for the coordinates of bovine PF4 and Professor Chris Hill for some of the data collection at the University of Utah. Acknowledgment is also given to Galvin Malenfant of the manufacturing group and Dr. Michael Kuranda from Process Development at Repligen for providing the protein samples. We are also grateful to Professor Alexander Rich at MIT for his helpful advice.

REFERENCES

Atkins, E. D. T., & Nieduszynski, I. A. (1976) *Heparin Chemistry and Clinic Usage* (Kakkar, V. V., & Thomas, D. P., Eds.) pp 21–35, Academic Press, New York.

Baldwin, E. T., Weber, I. T., Charles, R. St., Xuan, J.-C., Appella, E., Yamada, M., Matsushima, K., Edwards, B. F. P., Clore, G. M., Gronenborn, A. M., & Wlodawer, A. (1991) *Proc. Natl. Acad. Sci. U.S.A. 88*, 502–506.

Barber, A. J., Kaser-Glarzmann, R., Jakabora, M., & Luscher, C. (1972) *Biochim. Biophys. Acta 286*, 312–329.

Bjorkman, P. J., Saper, M. A., Samraoui, B., & Bennett, W. S. (1987) *Nature 329*, 506–512.

Bock, P. E., Luscombe, M., Marshall, S. E., Pepper, D. S., & Holbrook, J. J. (1980) *Biochem. J. 191*, 769–776.

Broekman (1975) *Haematologica 31*, 51–55.

Brunger, A. T., Karplus, M., & Petsko, G. A. (1989) *Acta Crystallogr. A45*, 50–61.

Clore, G. M., Appella, E., Yamada, M., Matsushima, K., & Gronenborn, A. M. (1990) *Biochemistry 29*, 1689–1696.

Cook, J. J., Niewiarowski, S., Yan, Z., Schaffer, L., Lu, W., Stewart, G. J., Mosser, D. M., Myers, J. A., & Maione, T. E. (1992) *Circulation 85*, 1102–1109.

Cowan, S. W., Bakshi, E. N., Machin, K. J., & Isaacs, N. W. (1986) *Biochem. J. 234*, 485–488.

Crowther, R. A., & Blow, D. W. (1967) *Acta Crystallogr. 23*, 544–548.

Denton, J., Lane, D. A., Thunberg, L., Slater, A. M., & Lindhal, U. (1983) *Biochem. J. 209*, 455–460.

Deuell, T .F., Senior, R. M., Chang, D., Griffin, G. L., Heinrickson, R. L., & Kaiser, E. T. (1981) *Proc. Natl. Acad. Sci. U.S.A. 78*, 4854–4587.

Fitzgerald, P. M. D. (1988) *J. Appl. Crystallogr. 21*, 273–278.

Handin, R. I., & Cohen, H. J. (1976) *J. Biol. Chem. 251*, 4273–4282.

Hermodson, M. A., Schmer, G., & Kurachi, K. (1977) *J. Biol. Chem. 252*, 6267–6279.

Hunt, A. J., Gray, G. S., Myers, J. A., & Maione, T. E. (1990) *FASEB J. 4*, A1991.

Ibel, K., Poland, G. A., Baldwin, J. P., Pepper, D. S., Luscombe, M., & Holbrook, J. J. (1986) *Biochim. Biophys. Acta 870*, 58–63.

Katz, I. R., Thorbecke, G. J., Bell, M. K., Yin, J.-Z., Clarke, D., & Zucker, M. B. (1986) *Proc. Natl. Acad. Sci. U.S.A. 83*, 3491–3495.

Kolber, D. L., & Maione, T. E. (1992) *FASEB J. 6*, A1359.

Lane, D. A., Denton, J., Thunberg, L., & Lindahl, U. (1984) *Biochem. J. 218*, 725–732.

Lattman, E. E., & Love, W. E. (1972) *Acta Crystallogr. B26*, 1854–1857.

Linhardt, R. J., Ampofo, S. A., Fareed, J., Hoppensteadt, D., Mulliken, J. B., & Folkman, J. (1992) *Biochemistry 31*, 12441–12445.

Luscombe, M., & Holbrook, J. J. (1983) in *Glycoconjugates* (Chester, A. M., Heinegard, D., Lundblad, A., & Svensson, S., Eds.) pp 818–819, Secretariat, Lund.

Maione, T. E., Gray, G. S., Petro, J., Hunt, A. J., Donner, A. L., Bauer, S. I., Carson, H. F., & Sharpe, R. J. (1990) *Science 247*, 77–79.

Matsushima, K., & Oppenheim, J. J. (1989) *Cytokine 1*, 2–13.

Mayo, K. H., & Chen, M.-J. (1989) *Biochemistry 28*, 9469–9478.

Michalski, R., Lane, D. A., Pepper, D. S., & Kakkar, V. V. (1978) *Br. J. Haematol. 38*, 561.

Morgan, F. J., Begg, F. S., & Chesterman, C. M. (1977) *Thromb. Haemostasis 38*, 231–235.

Myers, J. A., Gray, G. G., Peters, D. J., Grimaila, R. J., Hunt, A. J., Maione, T. E., & Mueller, W. T. (1991) *Protein Expression Purif. 2*, 136–143.

Sharpe, R. J., Byers, H. R., Scott, C. F., Bauer, S. I., & Maione, T. E. (1990) *JNCI, J. Natl. Cancer Inst. 82*, 848–852.

St. Charles, R., Walz, D. A., & Edwards, B. F. P. (1989) *J. Biol. Chem. 264*, 2092–2099.

Taylor, S., & Folkman, J. (1982) *Nature 297*, 307–312.

Walz, A., Peveri, P., Aschauer, H., & Baggiolini, M. (1987) *Biochem. Biophys. Res. Commun. 149*, 755–761.

Whitson, R. H., Jr., Wong, W. L., & Itakura, J. (1991) *J. Cell. Biochem. 47*, 31–42.

Zucker, M. B., Katz, I. R., Thorbecke, G. J., Milot, D. C., & Holt, J. (1989) *Proc. Natl. Acad. Sci. U.S.A. 86*, 7571–7574.